






# Deriving x-ray pulse duration from center-of-energy shifts in THz-streaked ionized electron spectra

MAREK WIELAND,<sup>1,2,\*</sup>  NIKOLAY M. KABACHNIK,<sup>3,4,5</sup>  MARKUS DRESCHER,<sup>1,2</sup> YUNPEI DENG,<sup>6</sup> YUNIESKI ARBELO,<sup>6</sup> NIKOLA STOJANOVIC,<sup>3,7</sup> BERND STEFFEN,<sup>3</sup> JULIANE ROENSCH-SCHULENBURG,<sup>3</sup> RASMUS ISCHEBECK,<sup>6</sup> ALEXANDER MALYZHENKOV,<sup>6</sup> EDUARD PRAT,<sup>6</sup>  AND PAVLE JURANIĆ<sup>6</sup>

<sup>1</sup>Universität Hamburg, Luruper Chaussee 149, 22761 Hamburg, Germany

<sup>2</sup>Center for Ultrafast Imaging, Luruper Chaussee 149, 22761 Hamburg, Germany

<sup>3</sup>Deutsches Elektronen-Synchrotron (DESY), Notkestrasse 85, 22603 Hamburg, Germany

<sup>4</sup>Skobeltsyn Institute of Nuclear Physics, Lomonosov Moscow State University, Moscow 119991, Russia

<sup>5</sup>Donostia International Physics Center (DIPC), E-20018 San Sebastian/Donostia, Spain

<sup>6</sup>Paul Scherrer Institut, 111 Forschungsstrasse, 5232 Villigen, Switzerland

<sup>7</sup>DLR-Institute for Optical Sensor Systems, Berlin 12489, Germany

\*marek.wieland@uni-hamburg.de

**Abstract:** A fast and robust, yet simple, method has been developed for the immediate characterization of x-ray pulse durations via IR/THz streaking that uses the center of energy (COE) of the photoelectron spectrum for the evaluation. The manuscript presents theory and numerical models demonstrating that the maximum COEs shift as a function of the pulse duration and compares them to existing data for validation. It further establishes that the maximum COE can be derived from two COE measurements set at a phase of  $\pi/2$  apart. The theory, model, and data agree with each other very well, and they present a way to measure pulse durations ranging from sub-fs to tens of fs on-the-fly with a fairly simple experimental setup.

© 2021 Optical Society of America under the terms of the [OSA Open Access Publishing Agreement](#)

## 1. Introduction

X-ray free electron laser (FEL) facilities have been in operation and used for experiments for over a decade [1–7], and the experience from conducting experiments at FEL sources is that pulse-to-pulse characterization of the photon beam is fundamental to be able to both optimize their performance, and analyze the experimental data. One important parameter is the pulse duration of each individual x-ray pulse, and a large number of methods have been implemented, tested, and published that aimed at providing beam synchronous values, like post-undulator electron beam transverse deflection structures (TDS) [8,9], spectral characterization of pulse duration via Fourier transforms [10–12], and THz or IR streaking [13–24]. The last set of methods is the one that is most capable of measuring the photon pulse duration directly, whereas post undulator TDS does not show the pulse duration after the optical elements in the FEL and is affected by artifacts in the electron beam, while the spectral evaluation methods suffer from a lack of knowledge about chirp, phase, and shape of the FEL pulse that should be known to get the correct values, and is limited by spectral imperfections.

The streaking method can provide the pulse duration near the experimental stations, thus enabling the pulse duration measurement after most or all optical elements in the beamline, but has some issues as well. It can yield wrong pulse durations, if a possible photon energy shift over time (chirp) is not adequately considered. The evaluation of streaking traces uses de-convolution from a non-streaked spectrum, which could be affected if there are substantial space-charge

issues. The width evaluations can also be difficult for non-Gaussian shaped beams, and getting a consistent number for the different FEL operation modes to represent the pulse duration can be difficult. More advanced attempts of evaluation, like [25] also require intense computation and many assumptions to get a consistent value.

This manuscript presents a different way of setting up and evaluating streaked spectra that has the potential to both give more consistent and more easily interpreted values, while also being less computationally demanding. The evaluation concentrates on the relationship between the center of energy (COE) of the streaked electron spectrum and the duration of the photon pulses, and how the former can be measured to derive the latter. Furthermore, the manuscript demonstrates under what conditions the maximum COE shift can be calculated from the streaked spectra and use this property to derive the pulse duration. Lastly, we will present experimental data that confirm these evaluations, and propose experimental setups that could fully utilize these properties. The model assumes that the temporal profile of the ionizing pulse is Gaussian, but it can also be adapted for any other arbitrary shape. The evaluation is simple, with very little computational cost, as described in section 2.2. The method also has the advantage of being applicable with a simple laser setup, usually using wavelengths that are reachable by laser harmonics or an optical parametric amplifier (OPA).

## 2. Theory

### 2.1. Classical model

The streaking process [14–17,22,23,25] observed in the polarization plane of the streaking field can be classically described by Eq. (1).

$$K_f = K_0 + 2U_p \sin^2(\omega t + \varphi) \pm \sqrt{8K_0 U_p} \sin(\omega t + \varphi) \cos \theta \quad (1)$$

$K_f$  is the final kinetic energy of the photoionized electron being streaked,  $K_0$  is the initial kinetic energy of the electron upon ionization,  $U_p$  is the ponderomotive energy,  $\omega$  is the angular frequency of the streaking field,  $t$  is the time when the electron was ionized in the field,  $\varphi$  is the phase of the field, and  $\theta$  is the angle between the polarization of the field and the direction of electron emission.  $U_p$  is described as

$$U_p = \frac{e^2 E_0^2}{4m_e \omega^2}, \quad (2)$$

where  $e$  is the electron charge,  $E_0$  the amplitude of the streaking electric field, and  $m_e$  the electron mass. If one concentrates solely on the change in the kinetic energy of the electron due to the streaking  $\Delta K$  in the direction of the electric field, one obtains:

$$\Delta K = 2U_p \sin^2(\omega t + \varphi) + \sqrt{8K_0 U_p} \sin(\omega t + \varphi). \quad (3)$$

The first term in Eq. (3) is usually ignored since  $K_0 \gg U_p$  and we will do so now to simplify the presentation, though the numerical model applied below takes the term into account:

$$\Delta K \cong \sqrt{8K_0 U_p} \sin(\omega t + \varphi). \quad (4)$$

If the half-period of the streaking field is significantly longer than the x-ray pulse duration, the effect is useful for getting temporal information about the x-ray pulse. The evaluation of the photoelectron spectra can reveal the arrival time of the x-ray pulse within a period of the streaking field, and the evaluation of the change in the width of the photoelectron peak can be used to estimate the pulse duration. However, experimental evaluations of pulse duration suffer from other possible sources of broadening of the photoelectron spectra, like space charge, x-ray beam chirp, device and methodology uncertainty, and noise.

A good example of a method-based uncertainty is the fitting of the peaks to get a width. Most often, this is done with Gaussian fits, but not all spectra are perfectly Gaussian, causing issues when attempting to compare every measured photoelectron spectrum to each other. This difficulty in the evaluations of pulse durations using the broadening of the peaks has led the authors to develop an alternate evaluation procedure that uses the shift of the center of energy (COE) as an indicator of pulse duration, described in the following sections.

## 2.2. Effects of pulse duration on the center of energy

In this section we show how the COE of the streaked electron spectrum is linked with the pulse duration. Here we follow the derivation presented in [24] (Supplementary Information). The shift of the COE of the electron spectrum, denoted as  $\delta C_K$ , can be written in the quantum mechanical model of streaking as

$$\delta C_K = \frac{\int \left( \frac{k^2}{2} - K_0 \right) W(k) k dk}{\int W(k) k dk}, \quad (5)$$

where  $k = \frac{p}{\sqrt{m_e}}$ , the electron momentum divided by the square root of its mass, and  $W(k)$  is the probability of the photoemission in the laser field. Assuming that the photoemission of the electrons can be considered instantaneous for most streaking experiments at FELs, with  $K_0 > 30$  eV one can use the Strong Field Approximation (SFA) [26] to derive an expression for  $W(\vec{k})$  [27]:

$$W(\vec{k}) = C \left| \int_{-\infty}^{\infty} dt \tilde{\epsilon}_X(t) D_{\vec{k}} e^{i\Phi_W(\vec{k}, t)} \right|^2. \quad (6)$$

$C$  is a constant that is irrelevant to the following discussion,  $\tilde{\epsilon}_X(t)$  is the envelope of the x-ray pulse,  $D_{\vec{k}}$  is the dipole matrix element describing the transition probability of an electron from the ground state to the continuum, and  $\Phi_W(\vec{k}, t)$  is related to the Volkov phase [28] accumulated by the electron moving through the streaking field. This phase can be written as

$$\Phi_W(\vec{k}, t) = - \int_t^{\infty} dt' \left[ \frac{1}{2} \left( \vec{k} - \frac{e}{\sqrt{m_e}} \vec{A}_s(t') \right)^2 - K_0 \right]. \quad (7)$$

$\vec{A}_s(t')$  is the vector potential of the streaking electric field  $\tilde{\epsilon}_s(t')$  defined by

$$\vec{A}_s(t') = - \int_{t'}^{\infty} dt'' \tilde{\epsilon}_s(t''). \quad (8)$$

Assuming a unity dipole matrix element and a Gaussian pulse shape for the x-ray field envelope, we define

$$G_X(t) \equiv \tilde{\epsilon}_X(t) D_{\vec{k}} \approx e^{-\frac{t^2}{2\sigma_E^2}}. \quad (9)$$

We also assume that the vector potential takes the simple form

$$\vec{A}_s(t) = \vec{A}_0(t) \cos(\omega t) \quad (10)$$

with a time-independent amplitude,  $\vec{A}_0(t) = \vec{A}_0$  and a period  $T = 2\pi/\omega$  being significantly longer than the x-ray pulse.

We now wish to calculate the effect that the pulse duration has on the maximum shift of the COE. Though this calculation can be done with the full quantum mechanical treatment, it is instructive to derive it with a semi-classical approximation of the quantum expression to more easily observe the link between the final energy of the electron and its moment of photoionization.

Calculating the exponential  $e^{i\Phi_W(\vec{k}, t)}$  in Eq. (6) is time-consuming because it varies rapidly with time. However, the fast oscillations of the integrand allow for the evaluation of the integral

of Eq. (6) around the points of stationary phase (saddle points)  $t_s$  where  $\frac{\partial \Phi_W(\vec{k}, t)}{\partial t}|_{t_s} = 0$ . This condition results in

$$(k^2/2 - K_0) - k \cos(\theta) A_s(t_s) + A_s^2(t_s)/2 = 0 \quad (11)$$

where  $k = |\vec{k}|$ , and  $A_s(t) = \frac{e}{\sqrt{m_e}} |\vec{A}_s(t)|$ . As a further simplification, we will assume that the detection of the electrons takes place along the polarization axis of the light field, and set  $\theta = 0$ . Equation (11) is analogous to Eq. (1), linking the time of ionization  $t_s$  with the final kinetic electron momentum  $k$  and the kinetic energy  $K_f = k^2/2$ .

Integrating Eq. (6) with the stationary phase method yields

$$W(k) = C |\Phi''(k, t_s)|^{-1} |G_X(t_s)|^2 \quad (12)$$

with  $\Phi''(k, t_s) = (k - A(t_s)) \frac{\partial A}{\partial t}|_{t=t_s}$  being the second derivative of the phase from Eq. (7) with respect to time at a stationary (saddle) point. Assuming that the experiment is set up such that  $A_0 \ll k$ ,  $k_0$ , as was done for Eq. (4), we can use Eq. (11) to get the identity

$$\frac{\partial A}{\partial t}|_{t=t_s} = \frac{\partial K}{\partial t}|_{t=t_s}. \quad (13)$$

Putting together the equations derived thus far, substituting Eq. (12) into Eq. (5) while using the relations in Eq. (11) and (13), the shift of the COE of the electron spectra can be written as

$$\delta C_K = k_0 \frac{\int A_s(t) G_X^2(t) dt}{\int G_X^2(t) dt} \quad (14)$$

with the script  $s$  being omitted from  $t_s$ .

We are interested in the behavior of the shift as a function of the duration  $\sigma$  of the Gaussian x-ray pulse. For any arbitrary arrival time  $t_0$  of the x-ray pulse along the slope of the streaking field, we can start from Eq. (14) and set

$$G_X^2(t) \approx e^{-(t-t_0)^2/\sigma_E^2}. \quad (15)$$

We keep the first three terms in the power series expansion of  $A_s(t)$  around  $t_0$  to get

$$A_s(t) = A_0(t_0) + \frac{\partial A_s}{\partial t}|_{t_0} (t - t_0) + \frac{1}{2} \frac{\partial^2 A_s}{\partial t^2}|_{t_0} (t - t_0)^2. \quad (16)$$

Evaluating Eq. (14) with definitions from Eq. (15) and (16), one realizes that the numerator in the second term is zero for a symmetric pulse. One gets the equation

$$\delta C_K \approx k_0 A_s(t_0) \left( 1 - \frac{1}{4} \omega^2 \sigma_E^2 \right). \quad (17)$$

It should be noted that Eq. (17) links the shift of the COE to the standard deviation  $\sigma_E$  of the electric field of the Gaussian x-ray pulse, not to  $\sigma_1$  of the photon intensity. A more useful evaluation for a lot of experiments is the intensity distribution of the photons in the pulse vs.

time, for which  $\sigma_E^2 = 2\sigma_I^2$ . Taking this into account, Eq. (17) becomes

$$\delta C_K \approx k_0 A_s(t_0) \left( 1 - \frac{1}{2} \omega^2 \sigma_I^2 \right). \quad (18)$$

For  $A_s(t) = A_0 \cos(\omega t + \varphi)$  and  $t_0 = t_{max}$ , the time at the maximum vector potential, this reduces to:

$$\delta C_K \approx k_0 A_0 \left( 1 - \frac{1}{4} \omega^2 \sigma_E^2 \right) \quad \text{and} \quad (19)$$

$$\delta C_K \approx k_0 A_0 \left( 1 - \frac{1}{2} \omega^2 \sigma_I^2 \right). \quad (20)$$

It should be noted that for  $|\vec{A}_s(t_0)| = E_0/\omega$ ,  $k_0 A_0 = \sqrt{8K_0 U_p}$ . Let us now consider the evaluation of Eq. (18) with two different phases offset from each other by  $\pi/2$ , such that  $\varphi' = \varphi + \pi/2$ . Inserting these two phase values into (17) leads to  $\delta C_K \approx k_0 A_0 \cos(\omega t + \varphi)$  and  $\delta C'_K \approx k_0 A_0 \cos(\omega t + \varphi') = k_0 A_0 \sin(\omega t + \varphi)$ . Using the trigonometric identity  $\sin^2 \theta + \cos^2 \theta = 1$ , one now quickly realizes that

$$\delta C_K^2 + \delta C'^2_K = \delta C_{K_{max}}^2 \quad (21)$$

being the maximum energy shift corresponding to  $t_0 = t_{max}$ .

The two main points to take away from the theory section are that: 1) the maximum COE of the streaked electron spectrum changes with the square of the pulse duration of the FEL pulse, and 2) one can derive the maximum shift of the COE from two measurements of the streaked spectra offset from each other by a phase difference of  $\pi/2$ . These two facts open the door for a simplified setup and evaluation procedure of this usually challenging measurement.

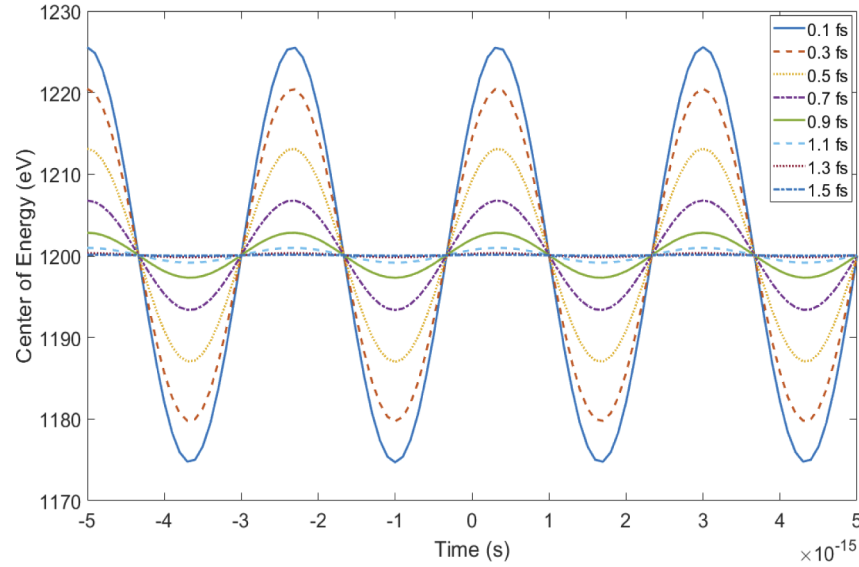
### 2.3. Numerical model

To obtain a more general idea about the strength of this method, and to move away from the assumption of the pulse duration being significantly smaller than the period of the streaking pulse that was used to derive Eq. (17) and (18), a numerical model was created that simulates the streaking process and extracts the COE values for a defined temporal x-ray profile, here chosen as a Gaussian distribution. This allows for following of the evolution of the method for longer pulse durations and in a multi-cycle streaking field, comparison of the model with Eq. (18) and (20), and evaluation of the applicability of the method to real experimental setups.

The model uses the classical equations to simulate the vector potential of the streaking pulse with variable pulse duration, wavelength, carrier envelope, and amplitude. The photoionized electrons were modeled to mirror the x-ray photon distribution and having a single kinetic energy to also match the theoretical approach. The assumption of a monochromatic x-ray pulse in the model makes no difference in the evaluation of the method's effectiveness since we are only concerned with a single energy, the COE of the electron spectrum. Effects from sideband formation [29,30] for longer pulse durations were ignored in the model because such effects are symmetric around the COE and would not contribute to the shift of the COE as long as  $U_p \ll K_0$ .

The model convolves the electrons generated from the x-ray pulse with the streaking field, effectively mapping the temporal distribution of the photons into a distribution along the energy axis, using the streaking equation (Eq. (1)) for the time-to-energy rescaling. The COE of the resulting spectrum is then calculated, and a map of the COE as the arrival time of the x-ray moves through the streaking field is extracted. This procedure is repeated for different pulse durations of the x-rays to visualize the change of the COE maximum value as a function of the pulse duration. The result is shown in Fig. 1 where 1200 eV photoelectrons are streaked in an 800 nm IR field. The parameters for the IR laser are 300 fs FWHM duration of the electric field envelope, 66  $\mu$ J

pulse energy, and a 250  $\mu\text{m}$  focus. For clarity, the figure concentrates only on a few of the cycles within the IR carrier envelope to show the effect of pulse duration on the maximum COE shift. The dependence of the maximum COE shift on the pulse duration is obvious.



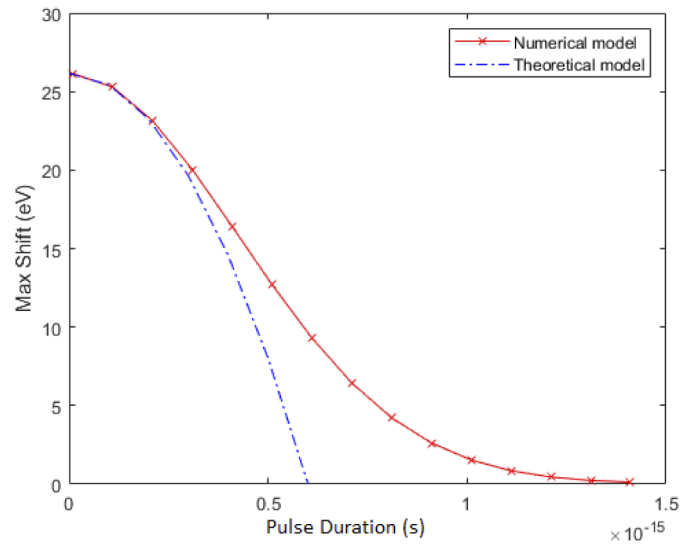
**Fig. 1.** The modeled COE evaluation of the shifted peaks of different pulse durations (inset legend) as the 1200 eV kinetic energy electrons become emitted at different times in an 800 nm IR field. The longer pulses result in smaller maximum shifts.

Figure 2 plots the shift of the COE from Eq. (18) at the maximum vector potential as a function of x-ray photon pulse duration, compared to the numerical model with the same settings for the amplitude of the electric field ( $3 \times 10^9$  V/m), streaking field wavelength (800 nm), and for different pulse durations. The agreement between the two approaches is very good for pulse durations of up to about  $\sigma = 0.35$  fs, which matches the theoretical model requirement of the period being much longer than the x-ray pulse. The theoretical and numerical model diverge beyond this point as expected, with the numerical model tracing the more complicated interaction of the x-ray pulse and the streaking field which begins to affect neighboring cycles. The theoretical model, with its simpler focus on the interaction of the x-ray pulse within the single cycle of the streaking field, goes to zero maximum shift fairly quickly. This is similar to the effect described in [29] for different lifetimes of Auger core-holes.

It is also self-evident from Fig. 1 that the COE trace as a function of time is sinusoidal, which is essential for the relationship  $\delta C_K^2 + \delta C_K'^2 = \delta C_{K_{max}}^2$ , described in section 2.1, to hold. The numerical and theoretical treatments of the COE evaluations agree very well with each other for pulse durations smaller than the laser half-period, they show that the maximum streaking COE is dependent on the pulse duration, and that the maximum COE can be evaluated from two measurements of the COE set at a phase difference of  $\pi/2$  apart. This means that an experiment is conceivable where the pulse duration can be determined from two simultaneous COE measurements of streaked electron spectra acquired in an appropriate geometry.

As mentioned earlier, the base model assumption is that the temporal profile of the ionizing radiation is Gaussian, which makes it ideal for a comparison to the theoretical model which also uses the same approximation. The assumption of a Gaussian shape is fairly common in the evaluation and estimation of pulse lengths, and holds true for transform-limited pulses, but actual SASE pulses may also be composed of multiple temporal spikes separated from each other. To show that the COE also changes with the length of such a spiky temporal profile, we have





**Fig. 2.** Comparison of the theoretical model according to Eq. (18) and the numerical model for COE shifts of sub-fs pulses for an 800 nm laser with peak electric field of  $3 \times 10^9$  V/m and electron kinetic energy of 1200 eV.

modified the numerical simulation such that the temporal duration of the ionizing pulse changes as we add more identical Gaussian pulse spikes separated by a set time. In this case, we used Gaussian pulses of 50 as rms width separated from each other by 200 as, added more and more of them, and evaluated the resulting COE shift in the same manner as for the single Gaussian pulse with a varying pulse length for the parameters from Fig. 1. The results presented in Fig. 3 show that the COE shift also decreases with pulse length, in a manner similar to the single-peak Gaussian case. Other values for rms widths and time separations were also modeled, all yielding similar trends. However, for the sake of space, we only present one of the worst-case scenario examples. The qualitative trend that longer pulse durations lead to a smaller COE offset follows, and even in this extreme case, still matches the standard Gaussian case for short pulse lengths, leading to a deviation of about 40% at 1.5 fs. For models that had peak structures still confined to a generally Gaussian envelope, the values matched the standard Gaussian model very closely.

Further simulations to generalize the applicability of the model were also studied, including a bandwidth of the kinetic energy of the ionized electrons, and also an energy chirp of the ionization process. The results were in some ways similar, as a chirp also imparts a spectral distribution on the electrons. The case presented in Fig. 1 was also evaluated with linear energy chirps of -10 eV/fs, -2 eV/fs, 2 eV/fs, and 10 eV/fs around the central energy of 1200 eV, with the spectral rms width of the electrons being equal to the chirp multiplied by the rms width of the temporal profile, resulting in spectra of between 0.2 and 15 eV rms width. For these cases, the resulting COE evaluations and shifts remained undistinguishable from the case with a single energy, giving plots whose difference from Fig. 1 and Fig. 2 were smaller than the width of the line used to plot them. This result should hold when the energy width of the spectrum is significantly smaller than the average kinetic energy of the photoelectrons, which is true at most FELs since their spectral bandwidth is typically orders of magnitude smaller than the photon energy [31].

This finding is not surprising. When  $K_0$  is substituted with  $K_0 + \delta K$  in Eq. (4), one can approximate  $\sqrt{K_0 + \delta K} = \sqrt{K_0} + 1/2 \delta K$  with a first order Taylor-McLaurin expansion for  $\delta K \ll K_0$ . The result is a linear and symmetric distribution of streaked photoelectron energies around the main streaked center energy, which preserves the COE evaluation.

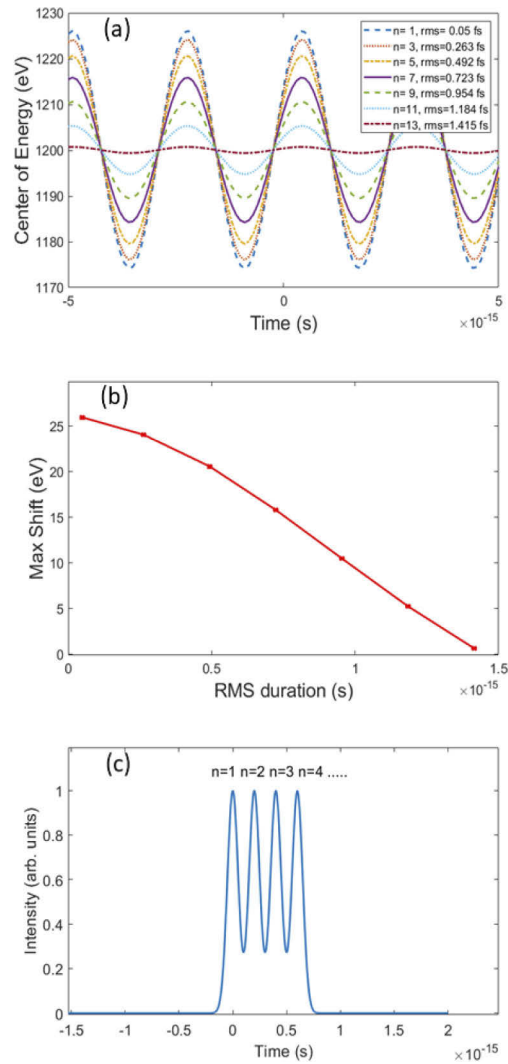


**Fig. 3.** The modeled COE evaluation for a spiky FEL pulse consisting of  $n$  Gaussian peaks (rms=50 as, separation=200 as). As before, the longer pulses result in smaller maximum shifts (a). The numerical model for COE shifts of the  $n$  Gaussian pulses for an 800 nm laser with peak electric field of  $3 \times 10^9$  V/m and electron kinetic energy of 1200 eV (b). An example of the used temporal pulse profile for  $n=4$  (c).



### 3. Proposal for pulse duration evaluation

If a FEL facility was interested in characterizing a new operation mode that could produce sub-fs level pulses, similar to those described in [11,12], a setup with two eTOFs can be used to measure the streak from a 800 nm laser (half-period of about 1.3 fs) interacting with ionized photoelectrons. To ensure that the FEL-laser jitter plays a negligible role in the evaluation, an 800 nm pulse that is significantly longer than the FEL-laser jitter has to be employed to ensure that the value of  $E_0$  and therefore also  $A_0$  does not change significantly over the jitter window of the FEL-laser interaction. For a laser pulse with a Gaussian carrier envelope, if one requires to have the variation in  $E_0$  to not exceed 5%, the ratio between the size of the jitter window and the rms width of the carrier pulse is about 0.64. For example, for jitter a window of 80 fs, the sigma of the electric field carrier envelope for the laser pulse should be larger than 125 fs width (300 fs FWHM). The laser pulse energy requirements for this sort of experiment would also be easily reachable, as the example in Fig. 1 shows. Furthermore, the large jitter window also means that there is no requirement on the laser carrier phase (CP) envelope stability, as the FEL-laser jitter is much larger than any jitter caused within the carrier envelope.

For the parameters in Fig. 1, namely 1200 eV electrons generated from an FEL pulse being streaked with an IR laser with 800 nm wavelength, 250  $\mu\text{m}$  focus, and a pulse duration (Gaussian carrier envelope) of 300 fs FWHM, the numerical model was used to calculate the expected data from such an experiment. It uses the COE  $\pi/2$  approach by evaluating the two values of the COE for every time step in an 80 fs jitter window with a phase offset of  $\pi/2$ , and then calculating the resulting expected maximum COE shift using Eq. (21). The results, along with expected sources of error, and the final accuracy of the measurements, are presented in Table 1. The expected sources of error are a combination of the jitter within the jitter window and the accuracy of measuring the COE of the spectra [17,24]. The uncertainty is dominated by the error in measurement of COE spectra, which is about 1.5 eV.

**Table 1. Modelled maximum COE evaluations ( $\delta C_{Kmax}$ ) of the COE  $\pi/2$  approach as a function of pulse duration ( $\sigma$ ) in as, with expected estimated error (Err. est.) and final uncertainty in the measurement for the case presented in Fig. 1 and above.**

$\sigma$ (as)	$\delta C_{Kmax}$ (eV)	Err. est. (eV)	Uncertainty (as)
100	25.0	1.55	77
200	23.0	1.54	51
300	20.0	1.53	43
400	16.5	1.52	42
500	12.8	1.51	45
600	9.44	1.51	53
700	6.58	1.50	67
800	4.34	1.50	92
900	2.70	1.50	136
1000	1.60	1.50	213
1100	0.89	1.50	360

The expected uncertainty for a 200 as pulse duration measurement would be about 50 as, and the method still delivers acceptable relative uncertainty even for 1000 as pulses, though it breaks down for pulse durations approaching the half of the streaking laser period. Also, the error in resolution becomes somewhat worse with extremely small pulse durations because of the square dependency of the COE shift on the pulse duration.

#### 4. Model validation with experimental data

The validation of the results from the theoretical COE model and the numerical simulation requires a check against experimental data. Preferably, the relationship between the maximum COE and the pulse duration can thus be proven. The main reason why this effect is non-trivial to deduce from most streaking experiments done at FELs is the arrival time jitter of the FEL vs. the streaking field. We first validate the numerical (and theoretical) model with available experimental data from FLASH where the FEL field and streaking fields were synchronized. We then, in the next section propose possible experimental setups in which the impact of the arrival time jitter can be excluded by properly choosing the e-TOFs geometry.

To be able to truly observe the COE of an electron spectrum in a vector potential to confirm the relationship shown in Eq. (18) and modelled in Fig. 1 one would need to repeat the experiment with several different pulse durations in a completely beam-synchronous way. Though the theory was developed for measurements of sub-fs pulse durations, it is also applicable to any pulse duration by scaling the streaking period accordingly. For tens of fs pulse durations, periods of  $\sim 100$  fs make THz radiation ideal for streaking.

The Free Electron Laser in Hamburg (FLASH) has a THz undulator [32] which provides THz radiation that is almost perfectly synchronized with the X-rays from the FEL. Since the same electron bunch is producing both the THz radiation and the FEL pulse, the synchronization of the two wavelengths to less than 5 fs root-mean-square (rms) [14] is possible. A THz streaking experiment was conducted at FLASH acquiring the electron time-of-flight (eTOF) spectra for FEL pulses of different durations as they were streaked through intense THz undulator radiation, thus providing a data set to test the theory with.

Krypton atoms were ionized with x-rays of mean photon energies of 176.5 eV and pulse energies between 1-10  $\mu$ J. The binding energies of the Kr 3d shells are 95.0 and 93.8 eV, resulting in kinetic energies of the electrons of about 81.5 and 82.7 eV, respectively. Two example spectra for an unstreaked and streaked case are shown in Fig. 4. Due to rather high FEL spectral bandwidth of about 1.5 eV rms, the spin-orbit splitting of the two photo-electrons is not resolved. The THz undulator was set up to deliver streaking fields with a wavelength of about 50  $\mu$ m, corresponding to a half-cycle of about 85 fs. Streaking spectrograms, i.e. electron spectra in dependence of the XUV-THz delay were recorded for two different pulse duration settings of the FEL. The extracted COEs for each delay are shown in Fig. 4 for both cases, representing the temporal evolution of the THz pulses. Their energy was measured to 0.76  $\mu$ J for the long pulses, and 0.94  $\mu$ J for the shorter ones, which corresponds to about 10% difference in the maximum electric field amplitude  $E_0$  between the two traces, which is typical for the performance of the FLASH THz undulator. The resolution of the delay stage allows a smallest delay step of  $\sim 17$  fs, and for each step the COE is determined by evaluating a mean spectrum of 30 shots.

Since the experiment does not provide an independent measurement of the vector potential, the exact values could not be used with Eq. (18) to validate the theory and derive an absolute pulse duration. The evaluation of the vector potential in a streaking experiment is usually done either by electro-optical (EO) sampling, or by using the streaking data to derive the vector potential from Eq. (4). Unfortunately, the very effect we notice, the shift in the COE, makes this evaluation impossible. Two different pulse lengths, streaked in the exact same vector potential, would give different streaking graphs and  $\Delta K$ . The shorter pulse length would be more correct, but it would still not give the real vector potential. Therefore, we are forced to evaluate the difference between them, using the shorter pulse as the baseline for the longer pulse.

If one designates the long pulse duration as  $\sigma_l$  and the short pulse duration as  $\sigma_s$ , they are related as  $\sigma_l^2 = \sigma_s^2 + \sigma_{conv}^2$  where  $\sigma_{conv}$  is a Gaussian pulse duration needed to be convolved with the short pulse duration to obtain the long one. Thus, the proper  $\sigma_{conv}$  necessary to convolve the COE trace of the short pulse to get the COE trace of the long pulse can be found. The approach makes sense when one realizes that the maximum COE of an infinitely short pulse (a delta

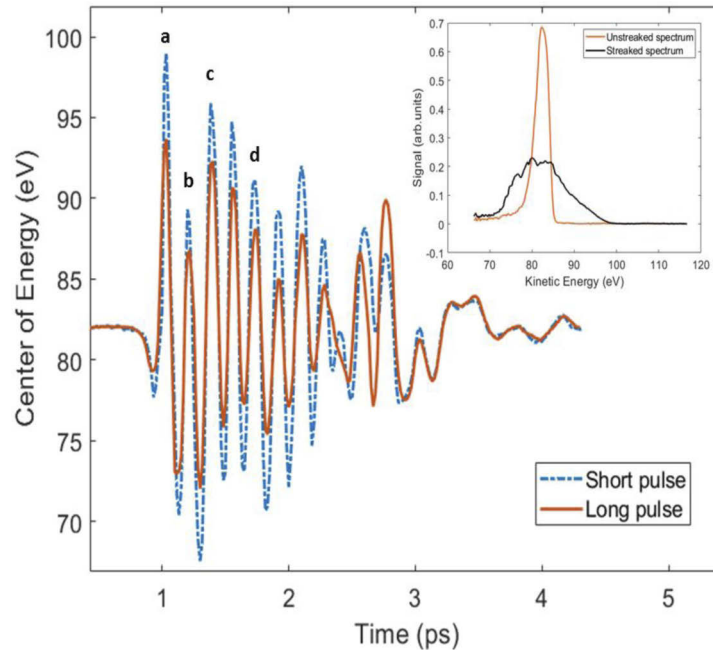


**Fig. 4.** COE evaluations of the long and short pulse duration THz traces from the experiment. The letters a, b, c, and d denote the cycles chosen for analysis. Inset: examples of unstreaked (red) and streaked (black) e-TOF single-shot spectra of the long pulse data.

function) is equal to  $k_0 A_0$ , as shown in Eq. (18), and any other duration COE we wish to evaluate can be thought of as the Gaussian pulse duration convolved with that delta function.

The evaluation of the data followed two approaches. The first one uses the standard pulse duration evaluation method from THz streaking as described in [14,33]. This evaluation fits the kinetic energy peaks of the streaked electrons to obtain their width,  $w_{streak}$ , at the largest slopes  $s$  (eV/fs) in the energy trace. The widths without streaking,  $w_0$  are deconvolved from the streaked widths and divided by the streaking speed, yielding the pulse duration  $\sigma_{time} = (w_{streak}^2 - w_0^2)^{1/2}/s$ . The streaking speeds are determined by fitting the COE trace curves with a linear fit around the point with the highest slope. As there was only one eTOF measuring the spectra, the effects of a chirp were ignored in the evaluations. The relative phase of the THz and XUV for the standard evaluation are chosen according to the steepest slope and biggest peak broadening, to make the evaluation of the pulse duration as straightforward as possible.

The second approach is based on our theoretical model described in the previous sections. It uses the convolution of the  $\sigma_s$  COE trace with a pulse of different duration  $\sigma_{conv}$  to obtain a trace that matches that of the one with pulse duration  $\sigma_l$  by matching their peak-to-peak heights. To this end, the COE streaking trace of the short pulse is convoluted with different duration Gaussian temporal profiles to find out which of the resulting COE traces best resembles the COE trace of the long pulse. The traces and convolutions are shown in Fig. 5 for the four different pulse slopes marked in Fig. 4. Ideally, the deconvolution of  $\sigma_s$  from  $\sigma_l$  derived from the standard evaluation should give the same value as  $\sigma_{conv}$  derived from the numerical model fit. The numerical model fit also considered the 10% difference between the electric field amplitude of the two traces. To ensure that the evaluations were as general as possible, multiple points along the different cycles of the streaking trace were chosen for the standard evaluation, and those same cycles were evaluated with the numerical model. The data for all cycles were averaged to give a meaningful comparison.

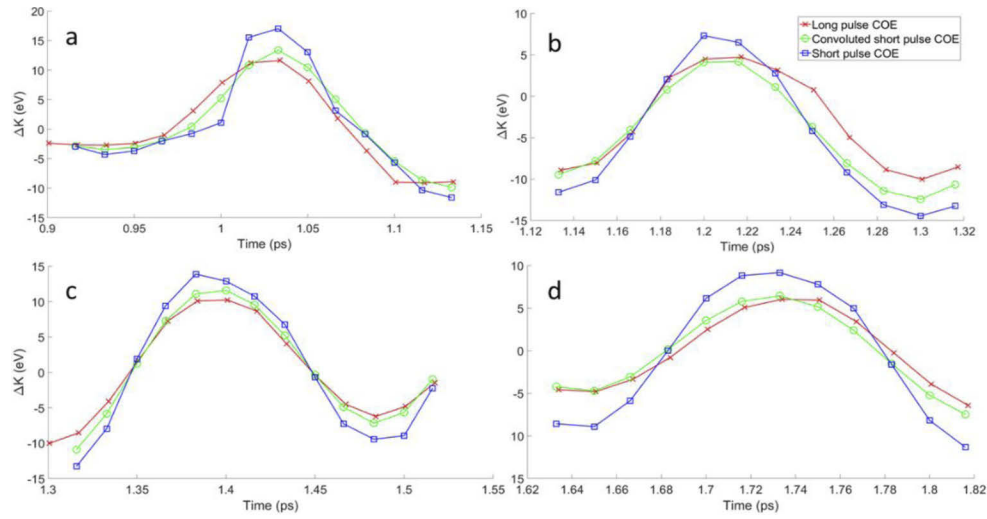


**Fig. 5.** Graphs of the traces for the short and long pulse COE traces, and the convolution of the short COE streaking trace with the appropriate  $\sigma_{conv}$  for cycles a, b, c, and d, as described in Fig. 4.

The results of the standard evaluation yielded  $\sigma_s = 19.5 \pm 4.0$  fs and  $\sigma_l = 23.9 \pm 2.7$  fs. The deconvolution of these two values leads to  $\sigma_{conv} = (\langle \sigma_l^2 \rangle - \langle \sigma_s^2 \rangle)^{1/2} = 17.0 \pm 6.1$  fs. The numerical modeling to find the best  $\sigma_{conv}$  for a Gaussian pulse duration to convolve with the short COE trace is shown in Fig. 4 and yielded a value of  $\langle \sigma_{conv} \rangle = 21.3$  fs with a standard deviation of 4.5 fs. It should be noted that the standard evaluation can be quite difficult, as even slight changes to starting parameters for width fits and background settings can have a large influence on the final evaluation. Similarly, the convolution of the short COE trace with a Gaussian pulse duration is somewhat limited by the spread of points in the dataset, as they were taken with a spacing of 17 fs. In light of these facts, the agreement between the above two values is quite good, showing that the relationships derived in section 2 hold.

## 5. Discussion on future experimental setups

Any future experiment intending to use the theoretical properties derived in this manuscript should, once the basic streaking is established, set up eTOFs such that they observe the same laser-FEL interaction with a phase difference of  $\pi/2$ . This can be achieved in many ways: from using the Gouy phase shift of a focused laser beam to observe different phases of the streaking field [18] (Fig. 6(a)), to circularly polarizing the streaking laser and placing two eTOFs at 90 degrees to each other and ensuring that they sample a small electron emission angle [20] (Fig. 6(b)), or using two separate setups with the laser beam separated and set up with a fixed phase difference to each other. Furthermore, the method is scalable. Though this approach was originally developed as a way to measure sub-fs pulses, the ratio of pulse duration to THz period ratio in the FLASH data also met the criteria for measurements. This means that as long as the order of magnitude of the pulse duration is known, the experiment can set up a streaking field to meet  $\tau_{x-ray} \ll \tau_{streak}$ . If no streak can be observed, then the current pulse duration is longer than expected, and either the streaking field or the pulse duration can be adapted.

For example, sub-fs pulses can easily be characterized using an 800 nm laser pulse, and longer pulse durations of 10-40 fs can easily be characterized using parametric amplifiers to create streaking fields with frequencies around 25 THz.

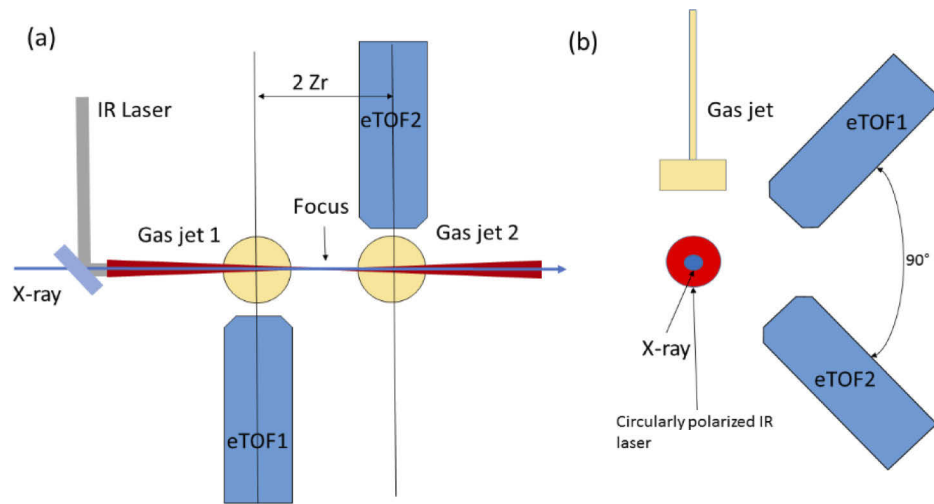


**Fig. 6.** Two possible setups for a COE evaluation experiment. Setup (a) uses the Gouy phase shift through a focus to get a fixed phase difference of  $\pi/2$  set at Rayleigh length ( $Z_r$ ) to the either side of the focus, whereas setup (b) looks at different phases of a circularly polarized streaking field.

Lastly, the proposed method is pulse-resolved. Since the information on the COE at the two different phases is retrievable for every single pulse, the pulse duration can be deduced on a shot-to-shot basis, with an error bar that would include the possible variations in  $E_0$ , the resolution of the eTOFs, and other experimental parameters. In addition, it should be noted that COE evaluations are much simpler and likely more accurate than the standard streaking spectrum width evaluations. Errors due to chirp and space charge effects are generally smaller for the COE evaluations as well. Therefore, real-time pulse duration measurements seem possible even for X-FELs operated up to MHz repetition rates.

## 6. Conclusion

The presented method of using the COE of the streaked photoelectron peak to characterize the x-ray pulse duration has demonstrated agreement between analytical theory, a numerical model, and experimental data. The approach allows for the evaluation of pulse durations from the sub-fs domain all the way up to more standard FEL pulses that are tens of fs long. The method is a powerful tool for simpler and easier pulse duration characterization that is less challenging in terms of laser setup, experiment, and evaluation, bringing it closer to something that could be routinely used with experiments and at facilities to help filter data or improve FEL operation set-up. Therefore it may help FEL facilities and other x-ray sources as they turn towards better time resolutions, and especially if future experiments require sub-fs pulses and temporal resolution.

**Funding.** Deutsche Forschungsgemeinschaft (SFB-925 – project 170620586); Deutsches Elektronen-Synchrotron; Donostia International Physics Center, DIPC (San Sebastian).

**Acknowledgments.** N.M.K. acknowledges the hospitality and financial support from DESY and from the theory group in cooperation with the SQS research group of the European XFEL (Hamburg), as well as the financial support from Donostia International Physics Center, DIPC (San Sebastian). M.W. and M.D. acknowledge funding by the Deutsche Forschungsgemeinschaft (DFG, German Research Foundation) – SFB-925 – project 170620586.

**Disclosures.** The authors declare no conflicts of interest related to this article.

**Data availability.** Data underlying the results presented in this paper are not publicly available at this time but may be obtained from the authors upon reasonable request.



## References

1. W. Ackermann, G. Asova, V. Ayvazyan, A. Azima, N. Baboi, J. Bahr, V. Balandin, B. Beutner, A. Brandt, A. Bolzmann, R. Brinkmann, O. I. Brovko, M. Castellano, P. Castro, L. Catani, E. Chiadroni, S. Choroba, A. Cianchi, J. T. Costello, D. Cubaynes, J. Dardis, W. Decking, H. Delsim-Hashemi, A. Delserieys, G. Di Pirro, M. Dohlus, S. Dusterer, A. Eckhardt, H. T. Edwards, B. Faatz, J. Feldhaus, K. Flottmann, J. Frisch, L. Frohlich, T. Garvey, U. Gensch, C. Gerth, C. Gorler, N. Golubeva, H. J. Grabosch, M. Grecki, O. Grimm, K. Hacker, U. Hahn, J. H. Han, K. Honkavaara, T. Hott, M. Huning, Y. Ivanisenko, E. Jaeschke, W. Jalmuzna, T. Jezynski, R. Kammering, V. Katalev, K. Kavanagh, E. T. Kennedy, S. Khodyachykh, K. Klose, V. Kocharyan, M. Korfer, M. Kollwe, W. Koprek, S. Korepanov, D. Kostin, M. Krassilnikov, G. Kube, M. Kuhlmann, C. L. S. Lewis, L. Lilje, T. Limberg, D. Lipka, F. Lohl, H. Luna, M. Luong, M. Martins, M. Meyer, P. Michelato, V. Miltchev, W. D. Moller, L. Monaco, W. F. O. Muller, A. Napieralski, O. Napoly, P. Nicolosi, D. Nolle, T. Nunez, A. Oppelt, C. Pagani, R. Paparella, N. Pchalek, J. Pedregosa-Gutierrez, B. Petersen, B. Petrosyan, G. Petrosyan, L. Petrosyan, J. Pfluger, E. Plonjes, L. Poletto, K. Pozniak, E. Prat, D. Proch, P. Pucyk, P. Radcliffe, H. Redlin, K. Rehlich, M. Richter, M. Roehrs, J. Roensch, R. Romaniuk, M. Ross, J. Rossbach, V. Rybnikov, M. Sachwitz, E. L. Saldin, W. Sandner, H. Schlarb, B. Schmidt, M. Schmitz, P. Schmuser, J. R. Schneider, E. A. Schneidmiller, S. Schnepp, S. Schreiber, M. Seidel, D. Sertore, A. V. Shabunov, C. Simon, S. Simrock, E. Sombrowski, A. A. Sorokin, P. Spanknebel, R. Spesyvtsev, L. Staykov, B. Steffen, F. Stephan, F. Stulle, H. Thom, K. Tiedtke, M. Tischer, S. Toleikis, R. Treusch, D. Trines, I. Tsakov, E. Vogel, T. Weiland, H. Weise, M. Wellhoffer, M. Wendt, I. Will, A. Winter, K. Wittenburg, W. Wurth, P. Yeates, M. V. Yurkov, I. Zagorodnov, and K. Zapfe, "Operation of a free-electron laser from the extreme ultraviolet to the water window," *Nat. Photonics* **1**(6), 336–342 (2007).
2. P. Emma, R. Akre, J. Arthur, R. Bionta, C. Bostedt, J. Bozek, A. Brachmann, P. Bucksbaum, R. Coffee, F. J. Decker, Y. Ding, D. Dowell, S. Edstrom, A. Fisher, J. Frisch, S. Gilevich, J. Hastings, G. Hays, P. Hering, Z. Huang, R. Iverson, H. Loos, M. Messerschmidt, A. Miahnahri, S. Moeller, H. D. Nuhn, G. Pile, D. Ratner, J. Rzepiela, D. Schultz, T. Smith, P. Stefan, H. Tompkins, J. Turner, J. Welch, W. White, J. Wu, G. Yocky, and J. Galayda, "First lasing and operation of an angstrom-wavelength free-electron laser," *Nat. Photonics* **4**(9), 641–647 (2010).
3. T. Ishikawa, H. Aoyagi, T. Asaka, Y. Asano, N. Azumi, T. Bizen, H. Ego, K. Fukami, T. Fukui, Y. Furukawa, S. Goto, H. Hanaki, T. Hara, T. Hasegawa, T. Hatsui, A. Higashiya, T. Hirono, N. Hosoda, M. Ishii, T. Inagaki, Y. Inubushi, T. Itoga, Y. Joti, M. Kago, T. Kameshima, H. Kimura, Y. Kirihaara, A. Kiyomichi, T. Kobayashi, C. Kondo, T. Kudo, H. Maesaka, X. M. Marechal, T. Masuda, S. Matsubara, T. Matsumoto, T. Matsushita, S. Matsui, M. Nagasono, N. Nariyama, H. Ohashi, T. Ohata, T. Ohshima, S. Ono, Y. Otake, C. Saji, T. Sakurai, T. Sato, K. Sawada, T. Seike, K. Shirasawa, T. Sugimoto, S. Suzuki, S. Takahashi, H. Takebe, K. Takeshita, K. Tamasaku, H. Tanaka, R. Tanaka, T. Tanaka, T. Togashi, K. Togawa, A. Tokuhisa, H. Tomizawa, K. Tono, S. K. Wu, M. Yabashi, M. Yamaga, A. Yamashita, K. Yanagida, C. Zhang, T. Shintake, H. Kitamura, and N. Kumagai, "A compact X-ray free-electron laser emitting in the sub-angstrom region," *Nat. Photonics* **6**(8), 540–544 (2012).
4. E. Allaria, D. Castronovo, P. Cinquegrana, P. Craievich, M. Dal Forno, M. B. Danailov, G. D'Auria, A. Demidovich, G. De Nino, S. Di Mitri, B. Diviacco, W. M. Fawley, M. Ferianis, E. Ferrari, L. Froehlich, G. Gaio, D. Gauthier, L. Giannessi, R. Ivanov, B. Mahieu, N. Mahne, I. Nikolov, F. Parmigiani, G. Penco, L. Raimondi, C. Scafuri, C. Serpico, P. Sigalotti, S. Spampinati, C. Spezzani, M. Svandrlik, C. Svetina, M. Trovo, M. Veronese, D. Zangrando, and M. Zangrando, "Two-stage seeded soft-X-ray free-electron laser," *Nat. Photonics* **7**(11), 913–918 (2013).
5. H. S. Kang, C. K. Min, H. Heo, C. Kim, H. Yang, G. Kim, I. Nam, S. Y. Baek, H. J. Choi, G. Mun, B. R. Park, Y. J. Suh, D. C. Shin, J. Hu, J. Hong, S. Jung, S. H. Kim, K. Kim, D. Na, S. S. Park, Y. J. Park, J. H. Han, Y. G. Jung, S. H. Jeong, H. G. Lee, S. Lee, S. Lee, W. W. Lee, B. Oh, H. S. Suh, Y. W. Parc, S. J. Park, M. H. Kim, N. S. Jung, Y. C. Kim, M. S. Lee, B. H. Lee, C. W. Sung, I. S. Mok, J. M. Yang, C. S. Lee, H. Shin, J. H. Kim, Y. Kim, J. H. Lee, S. Y. Park, J. Kim, J. Park, I. Eom, S. Rah, S. Kim, K. H. Nam, J. Park, J. Park, S. Kim, S. Kwon, S. H. Park, K. S. Kim, H. Hyun, S. N. Kim, S. Kim, S. M. Hwang, M. J. Kim, C. Y. Lim, C. J. Yu, B. S. Kim, T. H. Kang, K. W. Kim, S. H. Kim, H. S. Lee, H. S. Lee, K. H. Park, T. Y. Koo, D. E. Kim, and I. S. Ko, "Hard X-ray free-electron laser with femtosecond-scale timing jitter," *Nat. Photonics* **11**(11), 708–713 (2017).
6. E. Prat, R. Abela, M. Aiba, A. Alarcon, J. Alex, Y. Arbelo, C. Arrell, V. Arsov, C. Bacellar, C. Beard, P. Beaud, S. Bettoni, R. Biffiger, M. Bopp, H. H. Braun, M. Calvi, A. Cassar, T. Celcer, M. Chergui, P. Chevtsov, C. Cirelli, A. Citterio, P. Craievich, M. C. Divall, A. Dax, M. Dehler, Y. P. Deng, A. Dietrich, P. Dijkstal, R. Dinapoli, S. Dordevic, S. Ebner, D. Engeler, C. Erny, V. Esposito, E. Ferrari, U. Flechsig, R. Follath, F. Frei, R. Ganter, T. Garvey, Z. Q. Geng, A. Gobbo, C. Gough, A. Hauff, C. P. Hauri, N. Hiller, S. Hunziker, M. Huppert, G. Ingold, R. Ischebeck, M. Janousch, P. J. M. Johnson, S. L. Johnson, P. Juranic, M. Jurcevic, M. Kaiser, R. Kalt, B. Keil, D. Kiselev, C. Kittel, G. Knopp, W. Koprek, M. Laznovsky, H. T. Lemke, D. L. Sancho, F. Lohl, A. Malyzhenkov, G. F. Mancini, R. Mankowsky, F. Marcellini, G. Marinkovic, I. Martiel, F. Marki, C. J. Milne, A. Mozzanica, K. Nass, G. L. Orlandi, C. O. Loch, M. Paraliiev, B. Patterson, L. Patthey, B. Pedrini, M. Pedrozzi, C. Pradervand, P. Radi, J. Y. Raguin, S. Redford, J. Rehanek, S. Reiche, L. Rivkin, A. Romann, L. Sala, M. Sander, T. Schietinger, T. Schilcher, V. Schlott, T. Schmidt, M. Seidel, M. Stadler, L. Stingelin, C. Svetina, D. M. Treyer, A. Trisorio, C. Vicario, D. Voulout, A. Wrulich, S. Zerdane, and E. Zimoch, "A compact and cost-effective hard X-ray free-electron laser driven by a high-brightness and low-energy electron beam," *Nat. Photonics* **14**(12), 748–754 (2020).
7. W. Decking, S. Abeghyan, P. Abramian, A. Abramsky, A. Aguirre, and C. Albrecht, *et al.*, "A MHz-repetition-rate hard X-ray free-electron laser driven by a superconducting linear accelerator," *Nat. Photonics* **14**(6), 391–397 (2020).

8. Y. Ding, C. Behrens, P. Emma, J. Frisch, Z. Huang, H. Loos, P. Krejcik, and M. H. Wang, "Femtosecond x-ray pulse temporal characterization in free-electron lasers using a transverse deflector," *Phys. Rev. Spec. Top.-Accel. Beams* **14**(12), 120701 (2011).
9. C. Behrens, F. J. Decker, Y. Ding, V. A. Dolgashev, J. Frisch, Z. Huang, P. Krejcik, H. Loos, A. Lutman, T. J. Maxwell, J. Turner, J. Wang, M. H. Wang, J. Welch, and J. Wu, "Few-femtosecond time-resolved measurements of X-ray free-electron lasers," *Nat. Commun.* **5**(1), 3762 (2014).
10. Y. Inubushi, K. Tono, T. Togashi, T. Sato, T. Hatsui, T. Kameshima, K. Togawa, T. Hara, T. Tanaka, H. Tanaka, T. Ishikawa, and M. Yabashi, "Determination of the Pulse Duration of an X-Ray Free Electron Laser Using Highly Resolved Single-Shot Spectra," *Phys. Rev. Lett.* **109**(14), 144801 (2012).
11. S. Huang, Y. Ding, Y. Feng, E. Hemsing, Z. Huang, J. Krzywinski, A. A. Lutman, A. Marinelli, T. J. Maxwell, and D. Zhu, "Generating Single-Spike Hard X-Ray Pulses with Nonlinear Bunch Compression in Free-Electron Lasers," *Phys. Rev. Lett.* **119**(15), 154801 (2017).
12. A. Malyzhenkov, Y. P. Arbelo, P. Craievich, P. Dijkstal, E. Ferrari, S. Reiche, T. Schietinger, P. Juranic, and E. Prat, "Single- and two-color attosecond hard x-ray free-electron laser pulses with nonlinear compression," *Phys. Rev. Res.* **2**(4), 042018 (2020).
13. J. Itatani, F. Quere, G. L. Yudin, M. Y. Ivanov, F. Krausz, and P. B. Corkum, "Attosecond streak camera," *Phys. Rev. Lett.* **88**(17), 173903 (2002).
14. U. Fruhling, M. Wieland, M. Gensch, T. Gebert, B. Schutte, M. Krikunova, R. Kalms, F. Budzyn, O. Grimm, J. Rossbach, E. Plonjes, and M. Drescher, "Single-shot terahertz-field-driven X-ray streak camera," *Nat. Photonics* **3**(9), 523–528 (2009).
15. I. Grguras, A. R. Maier, C. Behrens, T. Mazza, T. J. Kelly, P. Radcliffe, S. Dusterer, A. K. Kazansky, N. M. Kabachnik, T. Tschentscher, J. T. Costello, M. Meyer, M. C. Hoffmann, H. Schlarb, and A. L. Cavalieri, "Ultrafast X-ray pulse characterization at free-electron lasers," *Nat. Photonics* **6**(12), 852–857 (2012).
16. W. Helml, A. R. Maier, W. Schweinberger, I. Grguras, P. Radcliffe, G. Doumy, C. Roedig, J. Gagnon, M. Messerschmidt, S. Schorb, C. Bostedt, F. Gruner, L. F. DiMauro, D. Cubaynes, J. D. Bozek, T. Tschentscher, J. T. Costello, M. Meyer, R. Coffee, S. Dusterer, A. L. Cavalieri, and R. Kienberger, "Measuring the temporal structure of few-femtosecond free-electron laser X-ray pulses directly in the time domain," *Nat. Photonics* **8**(12), 950–957 (2014).
17. P. N. Juranic, A. Stepanov, R. Ischebeck, V. Schlott, C. Pradervand, L. Patthey, M. Radovic, I. Gorgisyan, L. Rivkin, C. P. Hauri, B. Monoszai, R. Ivanov, P. Peier, J. Liu, T. Togashi, S. Owada, K. Ogawa, T. Katayama, M. Yabashi, and R. Abela, "High-precision x-ray FEL pulse arrival time measurements at SACLA by a THz streak camera with Xe clusters," *Opt. Express* **22**(24), 30004–30012 (2014).
18. W. Helml, I. Grguras, P. N. Juranic, S. Dusterer, T. Mazza, A. R. Maier, N. Hartmann, M. Ilchen, G. Hartmann, L. Patthey, C. Callegari, J. T. Costello, M. Meyer, R. N. Coffee, A. L. Cavalieri, and R. Kienberger, "Ultrashort Free-Electron Laser X-ray Pulses," *Appl. Sci.* **7**(9), 915 (2017).
19. I. Gorgisyan, R. Ischebeck, C. Erny, A. Dax, L. Patthey, C. Pradervand, L. Sala, C. Milne, H. T. Lemke, C. P. Hauri, T. Katayama, S. Owada, M. Yabashi, T. Togashi, R. Abela, L. Rivkin, and P. Juranic, "THz streak camera method for synchronous arrival time measurement of two-color hard X-ray FEL pulses," *Opt. Express* **25**(3), 2080–2091 (2017).
20. N. Hartmann, G. Hartmann, R. Heider, M. S. Wagner, M. Ilchen, J. Buck, A. O. Lindahl, C. Benko, J. Grunert, J. Krzywinski, J. Liu, A. A. Lutman, A. Marinelli, T. Maxwell, A. A. Miahnahri, S. P. Moeller, M. Planas, J. Robinson, A. K. Kazansky, N. M. Kabachnik, J. Viehhaus, T. Feurer, R. Kienberger, R. N. Coffee, and W. Helml, "Attosecond time-energy structure of X-ray free-electron laser pulses," *Nat. Photonics* **12**(4), 215–220 (2018).
21. A. K. Kazansky, I. P. Sazhina, and N. M. Kabachnik, "Fast retrieval of temporal characteristics of FEL pulses using streaking by THz field," *Opt. Express* **27**(9), 12939–12944 (2019).
22. R. Ivanov, I. J. B. Macias, J. Liu, G. Brenner, J. Roensch-Schulenburg, G. Kurdi, U. Fruhling, K. Wenig, S. Walther, A. Dimitriou, M. Drescher, I. P. Sazhina, A. K. Kazansky, N. M. Kabachnik, and S. Dusterer, "Single-shot temporal characterization of XUV pulses with duration from similar to 10 fs to similar to 350 fs at FLASH," *J. Phys. B: At., Mol. Opt. Phys.* **53**(18), 184004 (2020).
23. T. Oelze, O. Kulyk, B. Schutte, U. Fruhling, E. Klimesova, B. Jagielski, L. Dittrich, M. Drescher, R. Pan, N. Stojanovic, V. Polovinkin, K. P. Khakurel, K. Muehlig, I. J. B. Macias, S. Dusterer, B. Faatz, J. Andreasson, M. Wieland, and M. Krikunova, "THz streak camera performance for single-shot characterization of XUV pulses with complex temporal structures," *Opt. Express* **28**(14), 20686–20703 (2020).
24. D. C. Haynes, M. Wurzer, A. Schletter, A. Al-Haddad, C. Blaga, C. Bostedt, J. Bozek, H. Bromberger, M. Bucher, A. Camper, S. Carron, R. Coffee, J. T. Costello, L. F. DiMauro, Y. Ding, K. Ferguson, I. Grguras, W. Helml, M. C. Hoffmann, M. Ilchen, S. Jalas, N. M. Kabachnik, A. K. Kazansky, R. Kienberger, A. R. Maier, T. Maxwell, T. Mazza, M. Meyer, H. Park, J. Robinson, C. Roedig, H. Schlarb, R. Singla, F. Tellkamp, P. A. Walker, K. Zhang, G. Doumy, C. Behrens, and A. L. Cavalieri, "Clocking Auger electrons," *Nat. Phys.* **17**(4), 512–518 (2021).
25. S. Q. Li, Z. H. Guo, R. N. Coffee, K. Hegazy, Z. R. Huang, A. Natan, T. Osipov, D. Ray, A. Marinelli, and J. P. Cryan, "Characterizing isolated attosecond pulses with angular streaking," *Opt. Express* **26**(4), 4531–4547 (2018).
26. L. V. Keldysh, "Ionization in Field of a Strong Electromagnetic Wave," *Sov. Phys. JETP-USSR* **20**, 1307 (1965).
27. A. K. Kazansky, I. P. Sazhina, and N. M. Kabachnik, "Angle-resolved electron spectra in short-pulse two-color XUV plus IR photoionization of atoms," *Phys. Rev. A* **82**(3), 033420 (2010).
28. D. M. Wolkow, "Ueber eine Klasse von Loesungen der Diracschen Gleichung," *Z. Phys.* **94**(3-4), 250–260 (1935).



29. M. Drescher, M. Hentschel, R. Kienberger, M. Uiberacker, V. Yakovlev, A. Scrinzi, T. Westerwalbesloh, U. Kleineberg, U. Heinzmann, and F. Krausz, "Time-resolved atomic inner-shell spectroscopy," *Nature* **419**(6909), 803–807 (2002).
30. S. Dusterer, P. Radcliffe, C. Bostedt, J. Bozek, A. L. Cavalieri, R. Coffee, J. T. Costello, D. Cubaynes, L. F. DiMauro, Y. Ding, G. Doumy, F. Gruner, W. Helml, W. Schweinberger, R. Kienberger, A. R. Maier, M. Messerschmidt, V. Richardson, C. Roedig, T. Tschentscher, and M. Meyer, "Femtosecond x-ray pulse length characterization at the Linac Coherent Light Source free-electron laser," *New J. Phys.* **13**(9), 093024 (2011).
31. E. Prat, P. Dijkstal, E. Ferrari, and S. Reiche, "Demonstration of Large Bandwidth Hard X-Ray Free-Electron Laser Pulses at SwissFEL," *Phys. Rev. Lett.* **124**(7), 074801 (2020).
32. R. Pan, E. Zapolnova, T. Golz, A. J. Krmpot, M. D. Rabasovic, J. Petrovic, V. Asgekar, B. Faatz, F. Tavella, A. Perucchi, S. Kovalev, B. Green, G. Geloni, T. Tanikawa, M. Yurkov, E. Schneidmiller, M. Gensch, and N. Stojanovic, "Photon diagnostics at the FLASH THz beamline," *J. Synchrotron Radiat.* **26**(3), 700–707 (2019).
33. U. Fruhling, "Light-field streaking for FELs," *J. Phys. B: At., Mol. Opt. Phys.* **44**(24), 243001 (2011).